Binarization of Spectral Histogram Models: An Application to Efficient Biometric Identification

Anika Pflug, Christian Rathgeb, Ulrich Scherhag, Christoph Busch
da/sec - Biometrics and Internet Secrity Research Group
Hochschule Darmstadt
{anika.pflug, christian.rathgeb, ulrich.scherhag, christoph.busch}@cased.de

***Abstract*—Feature extraction techniques such as local binary patterns (LBP) or binarized statistical image features (BSIF) are crucial components in a biometric recognition system. The vast majority of relevant approaches employs spectral histograms as feature representation, i.e. extracted biometric reference data consists of sequences of histograms. Transforming these histogram sequences to a binary representation in an accuracy-preserving manner would offer major advantages w.r.t. data storage and efficient comparison.**

We propose a generic binarization for spectral histogram models in conjunction with a Hamming distance-based comparator. The proposed binarization and comparison technique enables a compact storage and a fast comparison of biometric features at a negligible cost of biometric performance (accuracy). Further, we investigate a serial combination of the binary comparator and histogram model-based comparator in a biometric identification system. Experiments are carried out for two emerging biometric characteristics, i.e. palmprint and ear, confirming the soundness of the presented technique.

***Index Terms*—ear Recognition, palm print recognition, biometrics, binarization, cascaded search**

I. Introduction

Biometrics is referred to as "automated recognition of individuals based on their behavioural and biological characteristics" [11]. For different biometric characteristics, e.g. face or palmprint [14], [23], the task of recognizing individuals can be reduced to texture modelling/ recognition tasks. In the past years, numerous holistic image analysis techniques, which are designed to construct local image descriptors which efficiently encode texture information of image regions, have been found to perform well in biometric recognition. However, biometric applications have to fulfil additional requirements which may not be met by texture recognition approaches. In particular, the representation of extracted features as vectors of spectral histograms requires a complex comparator and, thus, hampers biometric systems to be operated in identification mode which requires an exhaustive $1 : N$ comparison, where N represents the number of subjects registered with the system. In addition, the storage of biometric reference data (templates) on smart card chips, magnetic stripes, or 2D bar codes requires a highly compact representation of feature vectors.

In order to address the aforementioned issues we propose a generic binarization scheme for spectral histogram models. We evaluate this approach for palmprint and ear images, however our method is likely to work for any other N-class separation problem where spectral histogram models can be applied. In particular, this means that the input images should be segmented and normalized w.r.t. rotation and scale. In the presented approach coefficients of histogram-based feature vectors are binarized according to a statistical analysis, reducing the template size by an order of magnitude. Moreover, the most reliable bits are detected for each subject. We design a Hamming distance-based comparator for efficient pair-wise comparison, employing a bit-mask in order to only compare the most reliable bits of subjects within relevant regions. Due to a potential loss of information during binarization we also suggest to employ a serial combination of comparison subsystems based on binary feature vectors and spectral histogram models, in order to accelerate biometric identification. For this purpose binary templates are used for pre-screening the entire database, i.e. the original comparison subsystem is only applied for a short-list of top-ranked candidates. The effectiveness of this approach has already been demonstrated for other biometric characteristics, cf. [3], [8]. Experiments, which are conducted on the publicly available PolyU palmprint database and the UND-J2 ear database, show that the proposed system based on binarized feature vectors maintains accuracy comparable to systems where exhaustive search using a real-valued feature vector is applied for identity retrieval. To the authors' knowledge this work represents the first generic approach to binarizing spectral histogram models for the purpose of biometric recognition.

978-1-4799-8322-3/15/$31.00

II. Related Work

Spectral Histogram Models have been widely used in the field of biometrics. Prominent representatives include LBP [1], BSIF [13], local phase quantisation (LPQ) [2] or histograms of oriented gradients (HOG) [6]. Based on a sub-window-wise binary encoding of texture features, spectral histograms are extracted for a sub-window in order to retain a certain amount of spatial information. During recognition, sequences of histograms from a probe feature vectors are compared to reference histograms. A variety of approaches using edges, statistical models and holististic descriptors in combination with subspace projection were evaluated for both biometric characteristics [14], [15]. According to previous work, spectral histogram descriptors were found to yield good recognition performance for both, ear and palm print images [17], [19].

However, spectral histograms represent a rather in-efficient

representation of biometric reference data, requiring large template sizes (histogram bins have to be stored as non-binary values, e.g. integers, where in general a reasonable amount of bins is expected to remain unset) and comparators require complex calculations in order to estimated comparison scores, e.g. χ^2 distance. In order to provide a compact representation and fast comparison of biometric feature vectors different approaches have been proposed to obtain binary feature vectors from biometric characteristics, e.g. minutiae cylinder codes [4] or iris-codes [7].

When referring to workload reduction w.r.t. biometric identification, we coarsely distinguish three key approaches: (1) classification, (2) indexing, and (3) a serial combination of a computationally efficient and an accurate (but more complex) algorithm. Let N denote the number of subjects registered with a biometric system and w be the workload for a pair-wise comparison of two templates. Then the overall workload W for biometric identification is defined as $W = wN + \delta$, where δ summarizes any additional one-time costs, e.g. sorting of candidates. In case the entire feature space is divided into c classes (i.e. subsets), W can be reduced to $wN/c + \delta$, given that the registered subjects are equally distributed among all classes. For instance, in [12], [20] and [18] fingerprint and ear images are assigned to $c = 5$ and $c = 4$ classes, respectively. It is generally conceded that small intra-class and large inter-class variations as well as sufficient image quality represent essential preliminaries in order to achieve acceptable preselection error rates.

Biometric indexing aims at reducing the overall workload in terms of $\mathcal{O}$-notation. While an optimal indexing scheme would require a workload in $\mathcal{O}(1)$, existing approaches focus on reducing the workload to at least $\mathcal{O}(\log N)$, yielding $W = w\log(N)$. In the majority of cases this is achieved by introducing hierarchical search structures which tolerate a distinct amount of biometric variance. Most noticeable indexing schemes for iris and fingerprints have been presented in [9] and [5], respectively.

Within serial combinations computationally efficient algorithms are used to extract a short-list of $\mathcal{L}N$ most likely candidates, with $\mathcal{L} \ll 1$. Therefore, W is reduced to $\hat{w}N + w\mathcal{L}N$, where $\hat{w}$ is the workload of a pair-wise comparison of the computationally efficient algorithm, $\hat{w} \ll w$. In other words, identification is accelerated if $w(1-\mathcal{L}) > \hat{w}$ holds. In [8] and [3] $\mathcal{L}$ was reduced to $\sim$10% for iris and voice, respectively, significantly accelerating biometric identification. Compared to indexing and classification a serial combination of algorithms enables a more accurate operation of the resulting trade-off between computational effort and accuracy by setting an adequate threshold for $\mathcal{L}$.

III. Binarization of Spectral Histogram Models

In the following subsections we define the terminology used w.r.t. spectral histogram models and provide a detailed description of the proposed binarization, the corresponding comparator, and the resulting serial identification scheme.

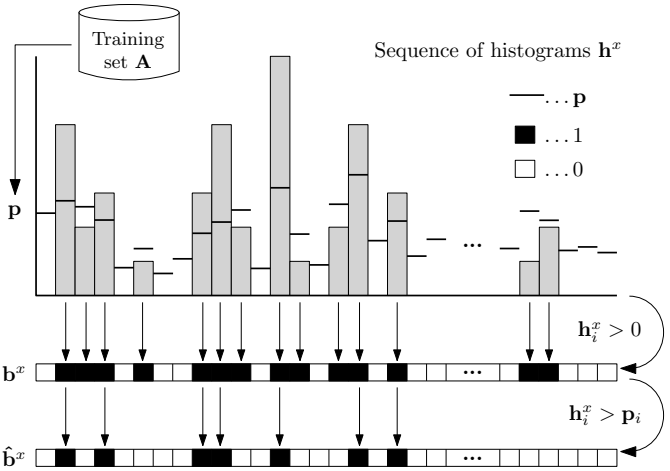

Fig. 1: Proposed binarization: two binary feature vectors are extracted out of a sequence of histogram coefficients.

A. Binarization

Given a preprocessed input image of subject x, we extract a sequence of n histogram coefficients $\mathbf{h}^x \in \mathbb{N}_0^n$. According to the employed sub-window dimension this sequence may consist of numerous fixed length spectral histograms. As mentioned earlier, the purpose of sub-windows in conjunction with spectral histogram features is to preserve spatial information within spectral histograms.

In the first step, $\mathbf{h}^x$ is binarized in order to obtain $\mathbf{b}^x \in \{0,1\}^n$ which points at all non-zero coefficients of $\mathbf{h}^x$,

$$\mathbf{b}^x_i = \begin{cases} 0, & \text{if } \mathbf{h}^x_i = 0 \\ 1, & \text{if } \mathbf{h}^x_i > 0. \end{cases} \tag{1}$$

As we will show in our experiments, the distribution of non-empty bins is discriminative for each subject. Depending on the particular settings, e.g. size of the local sub window or number of feature descriptor values, a significant amount of histogram bins can be expected to remain empty.

Using a training set $\mathbf{A}$ the mean-vector $\mathbf{p} \in \mathbb{R}^{n+}$ of all non-zero coefficients is estimated,

$$\mathbf{p}_i = \frac{\sum_{a\in\mathbf{A}} \mathbf{h}^a_i}{\sum_{a\in\mathbf{A}} \mathbf{b}^a_i}. \tag{2}$$

In the second step $\mathbf{h}^x$ is, again, binarized obtaining $\hat{\mathbf{b}}^x \in \{0,1\}^n$ in relation to the previously estimated $\mathbf{p}$,

$$\hat{\mathbf{b}}^x_i = \begin{cases} 0, & \text{if } \mathbf{h}^x_i \leq \mathbf{p}_i \\ 1, & \text{if } \mathbf{h}^x_i > \mathbf{p}_i. \end{cases} \tag{3}$$

The process of generating both binary vectors is schematically depicted in Fig. 1. We assume that for each subject $e > 1$ sample images are acquired during enrolment. Based on e acquisitions we calculate $\mathbf{p}^x$, $\boldsymbol{\sigma}^x \in \mathbb{R}^{n+}$, representing the subject-specific mean and variance vector, with $\boldsymbol{\sigma}^x_i = Var(\mathbf{p}^x_i)$. Then vector $\mathbf{r}^x \in \mathbb{R}_0^{n+}$, which defines the reliability

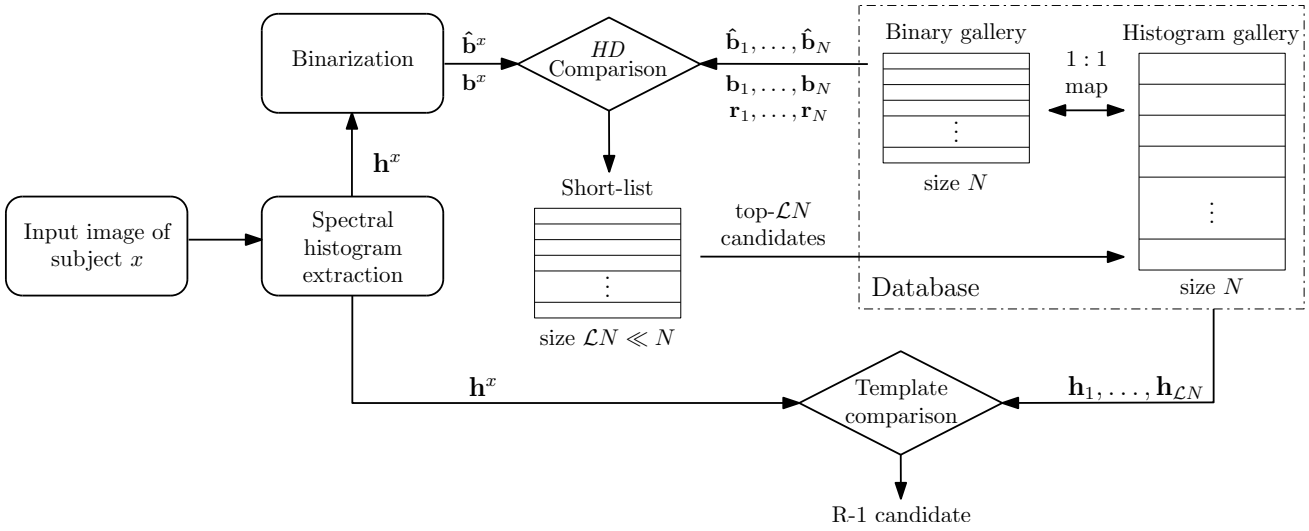

Fig. 2: Serial combination of computationally efficient and original comparator: the Hamming distance-based comparator is employed to perform an $1 : N$ comparison, returning a list of $\mathcal{L}N$ candidates on which the original comparator is applied.

of each coefficient, is defined as,

$$\mathbf{r}_i^x = \frac{\parallel \mathbf{h}_i^x - \mathbf{p}_i^x \parallel}{\boldsymbol{\sigma}_i^x}. \tag{4}$$

In other words, we identify those coefficients as reliable which are far from the mean (discriminative) and exhibit low variance (constant). Based on $\mathbf{r}^x$ we can obtain a binary vector $\mathbf{r}_k^x \in \{0,1\}^n$, pointing at the k most reliable bits of subject x.

B. Comparator

The (dis-)similarity $d(x,y)$ of a given probe sample $\mathbf{h}^y$ to a gallery template of subject x is finally defined as the fractional Hamming distance between binary feature vectors $\hat{\mathbf{b}}^x$ and $\hat{\mathbf{b}}^y$ deemed to the k most reliable bits of the gallery vector intersected with sets of non-zero coefficients,

$$d(x,y) = \frac{\parallel (\hat{\mathbf{b}}^x \oplus \hat{\mathbf{b}}^y) \cap \mathbf{r}_k^x \cap \mathbf{b}^x \cap \mathbf{b}^y \parallel}{\parallel \mathbf{r}_k^x \cap \mathbf{b}^x \cap \mathbf{b}^y \parallel}. \tag{5}$$

The XOR operator $\oplus$ detects disagreements between any corresponding pair of bits between the binary vectors $\hat{\mathbf{b}}^x$ and $\hat{\mathbf{b}}^y$. The result is intersected with the reliability mask $\mathbf{r}_k^x$ of the claimed identity x, i.e. the AND operator $\cap$ ensures that only the k most discriminative bits are used for comparison. Further, the resulting bit vector is intersected with $\mathbf{b}^x$ and $\mathbf{b}^y$ such that only relevant (non-zero) areas are considered at the time of comparison. Subsequently, the final score is normalized accordingly. The overlap mask is necessary, because we need to make sure that a probe and a reference feature vector have a sufficiently large and overlapping number of non-zero bins. The coefficient in these bins should have a small distance to the gallery feature vector.

It is important to note that the proposed comparator is highly efficient as it is only based on those two logical operators. It has been shown that Hamming distance-based comparators are capable of performing millions of comparisons per second [7].

C. Application to Serial Identification

Since the proposed binarization may cause a significant loss of biometric information and, thus, biometric performance, binarized templates can be alternatively used in a serial combination in order to accelerate identification. In this case the computational efficient Hamming distance-based comparator is utilized to pre-screen the entire database. For this purpose N pair-wise comparisons are performed, resulting in a vector $\mathbf{D}$ of dissimilarity scores, sorted in descending order $\mathbf{D} = (d_1 \leq d_2 \leq \cdots \leq d_N)$ where d_i denotes the score between the query and the i-th enrolment data record. Finally, the top-$\mathcal{L}N$ candidates, i.e. the candidates which the first $\mathcal{L}N$ scores in $\mathbf{D}$ point at, are returned.

Based on the short-list returned in the pre-screening stage the probe is compared against a fraction of $\mathcal{L}N$ original gallery templates applying a more complex comparator, e.g. Euclidean distance or χ^2 distance. The entire process is depicted in Fig. 2.

Based on the terminology defined in Sect. II, we assume that $\hat{w} \ll w$. By defining a speed-up factor $\alpha = w/\hat{w}$, we can estimate the maximum list size $\mathcal{L}$ such that $\hat{w}N + w\mathcal{L}N < wN$ still holds, yielding $\mathcal{L} \leq 1 - 1/\alpha$ (assuming that additional one-time costs are comparable for both systems). For example, if the pre-screener is 5 times faster than the original comparator the $\mathcal{L}$ should be significantly smaller than 80% of the entire number of registered subjects in order to obtain a substantial speed-up.

IV. Experimental Evaluations

In the following subsections we describe the setup of conducted experiments and report the performance of the proposed approach as well as a serial combination of comparators with respect to accuracy and identification speed.

TABLE I: Properties of the Poly-U palmprint datbase and the UND-J2 ear database and the number of resulting identification attempts.

Dataset Dataset	Number of Subjects	Number of Images	Image Resolution	Number of Identifications
Poly-U	250	6000	128×128	500
UND-J2	312	1536	100×100	312

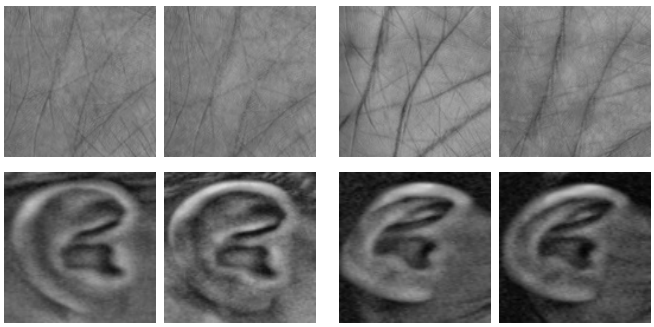

Fig. 3: Sample images of two subjects of the Poly-U palmprint datbase (top row) and two subjects of the UND-J2 ear database (bottom row).

A. Experimental Setup

Experiments are carried out on two different databases, the Poly-U palmprint database[1] [22] and the UND-J2 ear database[2] [21]. Properties of these datasets are summarized in Table I. We use four images per subjects for enrolment and the remaining images for performance evaluation. ROIs of the palm print images from PolyU are already segmented and normalized, such that we can extract the feature vectors without any additional preprocessing. For the UND-J2 dataset, which is acquired from a specified distance and contains slight variations in pose, we perform an automated normalisation process using Cascaded pose regression. The normalization algorithm was trained using images of 92 subjects. For more details on the preprocessing toolchain for ear images we refer the reader to [16]. Fig. 3 shows some examples for the palmprint images from PolyU and the segmented and normalized ear images from UND-J2.

Performance is estimated in terms of (true-positive) identification rate (IR). In accordance to the ISO/IEC IS 19795-1 [10] the IR is the proportion of identification transactions by subjects enrolled in the system in which the subject's correct identifier is the one returned. In experiments identification is performed in the closed-set scenario returning the rank-1 candidate as identified subject (without applying a decision threshold). Further, focusing on the serial combination of the binary system and the original one we report the penetration rate as the pre-chosen value $\mathcal{L}$ and the pre-selection error denoted by $\mathcal{P}$, defined as the error that occurs when the corresponding enrolment template is not in the preselected subset of candidates when a sample from the same biometric characteristic on the same user is given. We define the hit-rate of a system as $1 - \mathcal{P}$ for a chosen value of $\mathcal{L}$.

[1]Publicly available at http://www4.comp.polyu.edu.hk/~biometrics/MultispectralPalmprint/MSP.htm

[2]Publicly available at http://www3.nd.edu/~cvrl/CVRL/Data_Sets.html

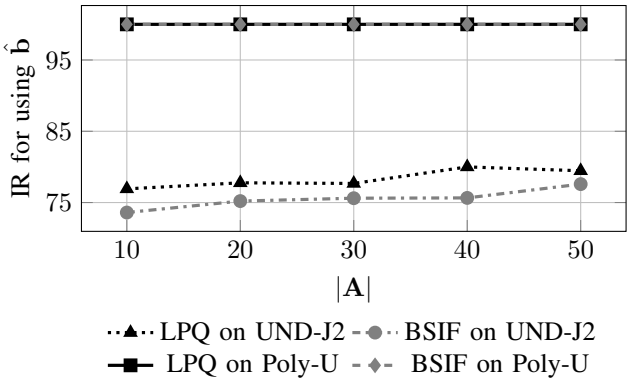

Fig. 4: IR for different numbers of training subjects $|\mathbf{A}|$ using only the vectors $\hat{\mathbf{b}}$s which are binarized according to the obtained mean vector $\mathbf{p}$.

In the feature extraction stage we use LPQ and BSIF as representatives for spectral histogram features, for further details on these algorithms the reader is referred to [2], [13]. Both feature extractors use 20×20 pixel sub windows with an overlap of 15 pixels between neighbouring windows. LPQ is computed with a radius of 3 pixels and BSIF is using a 5×5 pixel filter. This results in a fixed length histogram feature vectors comprising 20736 and 9216 histogram coefficients for both databases for the LPQ and the BSIF feature vectors, respectively. At the time of comparison of spectral histogram features we employ the χ^2-distance which estimates the normalized quadratic distance between histogram coefficients of fixed length vectors.

Finally, we choose a suitable size for the training set $\mathbf{A}$ used to generate the mean vector $\mathbf{p}$. For this purpose we estimate the IR for different training set sizes using only the vectors $\hat{\mathbf{b}}$s which are binarized according to the resulting mean vectors. As shown in Fig. 4, for the favourable Poly-U dataset a training set size of $|\mathbf{A}| = 10$ already reveals a perfect system (IR=100%). However, for the more unconstrained UND-J2 IRs improve with an increased $|\mathbf{A}|$, i.e. we identify $|\mathbf{A}| = 50$ as a suitable choice for both datasets.

B. Histograms vs. Binarized Features

For the LPQ feature extraction the original systems based on histogram features and the χ^2-distance yield a baseline performance of IRs of 100% and 83.05% for the Poly-U and the UND-J2 dataset, respectively. By analogy for the BSIF feature extraction we obtain IRs of 100% and 81.6%. We also tested the Euclidean distance as an alternative comparator, however, it was outperformed by χ^2-distance in all experiments. We observed that binary comparison is α =10.61 times faster than χ^2 and α =7.61 times faster than the Euclidean distance in our C++ implementation of the system. Table II summarizes the biometric performance in terms of IR and rank-$\mathcal{L}$ identification

TABLE II: Identification rates and hit rates for various values of $\mathcal{L}$ (in %) for PolyU-MS (top) and UND-J2 (bottom) and feature extraction algorithms using k most reliable bits during comparison.

k	IR	$\mathcal{L}$=5	$\mathcal{L}$=10	$\mathcal{L}$=30	$\mathcal{L}$=40	$\mathcal{L}$=50	k	IR	$\mathcal{L}$=5	$\mathcal{L}$=10	$\mathcal{L}$=20	$\mathcal{L}$=30	$\mathcal{L}$=50
PolyU-MS with LPQ							**PolyU-MS with BSIF**						
1%	69.11	97.33	99.33	100.0	100.0	100.0	1%	52.44	93.78	97.56	99.11	100.0	100.0
2%	88.67	99.33	99.78	100.0	100.0	100.0	2%	75.33	98.67	99.56	100.0	100.0	100.0
3%	91.33	99.56	100.0	100.0	100.0	100.0	3%	84.00	99.11	100.0	100.0	100.0	100.0
5%	96.22	99.78	100.0	100.0	100.0	100.0	5%	88.00	99.78	99.78	99.78	100.0	100.0
7%	97.77	99.78	100.0	100.0	100.0	100.0	7%	93.78	100.0	100.0	100.0	100.0	100.0
10%	98.22	100.0	100.0	100.0	100.0	100.0	10%	97.11	100.0	100.0	100.0	100.0	100.0
30%	99.78	100.0	100.0	100.0	100.0	100.0	30%	99.33	100.0	100.0	100.0	100.0	100.0
100%	100.0	100.0	100.0	100.0	100.0	100.0	100%	100.0	100.0	100.0	100.0	100.0	100.0
UND-J2 with LPQ							**UND-J2 with BSIF**						
1%	36.03	66.67	78.38	91.89	94.59	97.29	1%	52.68	71.43	78.57	89.29	95.54	98.21
2%	47.37	64.91	80.70	94.74	98.25	99.12	2%	56.64	72.57	84.07	94.69	96.46	99.11
3%	61.40	78.95	83.33	92.11	96.49	100.0	3%	46.85	69.34	81.08	90.99	93.69	99.10
5%	64.66	81.90	91.38	98.28	100.0	100.0	5%	62.39	76.15	86.24	96.33	98.17	98.17
7%	61.54	77.78	86.32	98.29	100.0	100.0	7%	63.79	78.44	87.93	96.55	97.41	99.14
10%	52.99	78.63	90.60	96.58	99.14	100.0	10%	65.52	76.72	81.03	93.10	95.67	99.14
30%	63.48	78.26	89.57	99.13	100.0	100.0	30%	65.79	79.82	86.84	94.74	98.25	100.0
100%	73.15	84.26	90.74	95.37	98.15	99.07	100%	78.38	84.68	90.99	96.39	99.10	99.10

rate which corresponds to $1-\mathcal{P}$ for binarized vectors obtained from both datasets using both feature extractors for various $\mathcal{L}$s and amounts of reliable bits, ks. For the Poly-U dataset (upper half of Table II) the proposed binarization technique maintains the biometric performance of IR=100% for both feature extraction algorithms. Further, we observe that the amount of employed bit comparison can be reduced to k =30% of most reliable bits maintaining comparable biometric performance. At higher ranks, e.g. $\mathcal{L}$ =30%, hit-rates of 100% are obtained even for comparing k =1% of most reliable bits.

On the more challenging UND-J2 dataset (lower half of Table II) the proposed binarization technique suffers from a significant loss of biometric information. However, at higher ranks, reasonable hit-rates are obtained for both feature extractors as shown in the cumulative match score distribution (CMC) curves plotted in Fig. 5 for k =30%. The binarized feature vectors achieve a comparable performance w.r.t. the original system at ranks of approximately 10-15%. That is, for the challenging UND-J2 dataset we identify the proposed binarization technique as a suitable candidate for an efficient pre-screener in a serial combination of algorithms. Further, the need for employing both types of binarized feature vectors is underlined, as the sole use of $\hat{\mathbf{b}}$ reveals significantly inferior results for both feature extractors compared to the proposed combination of $\mathbf{b}$ and $\hat{\mathbf{b}}$.

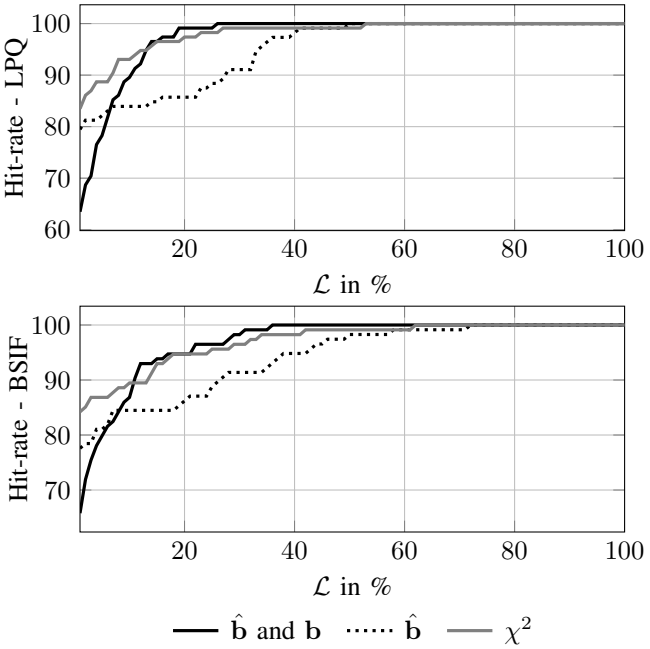

Fig. 5: CMC curves of the proposed binarizations compared to the original systems.

C. Serial Identification

In our second experiment, we apply the proposed binarization technique in a serial combination on the UND-J2 dataset (see Sect. III-C). We use the best configurations from the previous experiments and use them for generating the short list of $\mathcal{L}N$ candidates. We then re-order this short-list using the χ^2-distance on the original histogram-based templates and return the IR of the re-ordered list. The performance of the serial identification system is hence reported as a function of $\mathcal{L}$ and the IR of the re-ordered list which is depicted in Fig. 6 for both feature extraction algorithms. The IR of the serial identification system reaches it's maximum for list sizes between $\mathcal{L}$ =10-30% of the dataset. Based on the previously estimated speed-up factor of α =10.61 our short list has to be significantly smaller than 90% of the entire dataset in order to achieve a substantial speed-up compared to an full $1:N$ search using histogram-based feature vectors. Given this, we

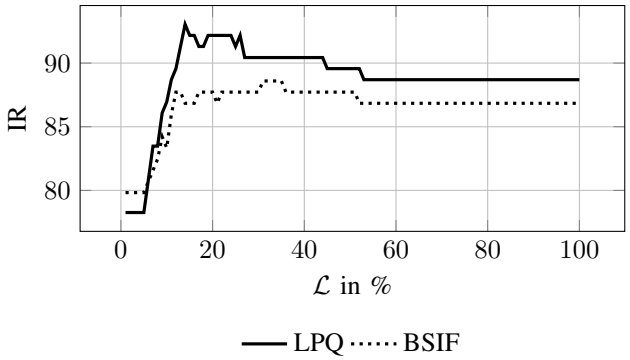

Fig. 6: IR of the serial identification system for different values of $\mathcal{L}$.

can conclude that the proposed serial identification system can perform an exhaustive search in 30% of the time compared to an exhaustive search using the χ^2-distance.

When comparing the IR of the serial identification system with the reference IR in Fig. 5, we can also see that the serial identification system outperforms the reference system that does an exhaustive $1 : N$ search using the χ^2-distance. This increase in performance is achieved due to the fact that the proposed system already discards candidates in the pre-screening stage which would have been falsely identified by the original system within an exhaustive search.

V. Conclusions

In this paper we have presented a generic binarization scheme for holistic spectral histogram descriptors and provided empirical results on two datasets and two different texture descriptors. The binary feature vectors are directly computed from the histogram representation and hence do not require an additional feature extraction. The proposed binarization technique can be used to reduce the size of biometric reference data and to perform efficient identification. We do not require an additional processing step for acquiring a binary representation of the feature vectors. Instead, we compute a binary representation directly from the spectral histogram descriptors.

The proposed method can be applied to all images, where a spectral histogram feature vector is used. In cases, where we have accurately segmented and registered images, the binary feature vector can be directly applied without a loss in biometric performance. On datasets acquired in a less constraint environment we suggest to employ the proposed system as pre-screener in a serial identification system in order to accelerate search operations. We found that the serial identification system even outperforms an exhaustive search of the original system.

Acknowledgements

This work is partially funded by the Federal Ministry of Education and Research of Germany and the Center for Advanced Security Research Darmstadt.

References

[1] T. Ahonen, A. Hadid, and M. Pietikainen. Face description with local binary patterns: Application to face recognition. *Pattern Analysis and Machine Intelligence, IEEE Transactions on*, 28(12):2037–2041, Dec 2006.

[2] T. Ahonen, E. Rahtu, V. Ojansivu, and J. Heikkila. Recognition of blurred faces using local phase quantization. In *19th International Conference on Pattern Recognition*, pages 1–4, Dec 2008.

[3] S. Billeb, C. Rathgeb, M. Buschbeck, H. Reininger, and K. Kasper. Efficient two-stage speaker identification based in universal background models. In *Intl. Conference of the Biometrics Special Interest Group*, 2014.

[4] R. Cappelli, M. Ferrara, and D. Maltoni. Minutia cylinder-code: A new representation and matching technique for fingerprint recognition. *Pattern Analysis and Machine Intelligence, IEEE Transactions on*, 32(12):2128–2141, Dec 2010.

[5] R. Cappelli, M. Ferrara, and D. Maltoni. Fingerprint indexing based on minutia cylinder-code. *Pattern Analysis and Machine Intelligence, IEEE Transactions on*, 33(5):1051–1057, May 2011.

[6] N. Dalal. *Finding Peple in Images and Vides*. PhD thesis, Institut National Polytechnique de Grenoble, 2006.

[7] J. Daugman. How iris recognition works. *Circuits and Systems for Video Technology, IEEE Transactions on*, 14(1):21–30, Jan 2004.

[8] J. Gentile, N. Ratha, and J. Connell. An efficient, two-stage iris recognition system. In *Biometrics: Theory, Applications, and Systems, 2009. BTAS '09. IEEE 3rd International Conference on*, pages 1–5, Sept 2009.

[9] F. Hao, J. Daugman, and P. Zielinski. A fast search algorithm for a large fuzzy database. *Trans. Info. For. Sec.*, 3(2):203–212, June 2008.

[10] ISO/IEC JTC1 SC37 Biometrics. *ISO/IEC 19795-1:2006. Information Technology – Biometric Performance Testing and Reporting – Part 1: Principles and Framework*. International Organization for Standardization and International Electrotechnical Committee, Mar. 2006.

[11] A. Jain, A. Ross, and S. Prabhakar. An introduction to biometric recognition. *Circuits and Systems for Video Technology, IEEE Transactions on*, 14(1):4–20, Jan 2004.

[12] A. K. Jain, S. Prabhakar, and L. Hong. A multichannel approach to fingerprint classification. *IEEE Trans. Pattern Anal. Mach. Intell.*, 21(4):348–359, Apr. 1999.

[13] J. Kannala and E. Rahtu. Bsif: Binarized statistical image features. In *IEEE International Conference on Pattern Recognition*, pages 1363–1366, 2012.

[14] A. Kong, D. Zhang, and M. Kamel. A survey of palmprint recognition. *Pattern Recognition*, 42(7):1408 – 1418, 2009.

[15] A. Pflug and C. Busch. Ear biometrics: a survey of detection, feature extraction and recognition methods. *Biometrics, IET*, 1(2):114–129, June 2012.

[16] A. Pflug and C. Busch. Segmentation and normalization of human ears using cascaded pose regression. In *19th Nordic Conference on Secure IT Systems*, 2014.

[17] A. Pflug, P. Paul, and C. Busch. A comparative study on texture and surface descriptors for ear biometrics. In *Proceedings of the International Carnahan Conference on Security Technology (ICCST)*, 2014.

[18] A. Pflug, A. Ross, and C. Busch. 2d ear classification based on unsupervised clustering. In *International Joint Conferent on Biometrics (IJCB)*, 2014.

[19] P. Promila and V. Laxmi. Palmprint matching using lbp. In *Computing Sciences (ICCS), 2012 International Conference on*, pages 110–115, Sept 2012.

[20] N. Ratha, K. Karu, S. Chen, and A. Jain. A real-time matching system for large fingerprint databases. *Pattern Analysis and Machine Intelligence, IEEE Transactions on*, 18(8):799–813, Aug 1996.

[21] P. Yan and K. W. Bowyer. An automatic 3d ear recognition system. In *3DPVT'2006*, pages 326–333, 2006.

[22] D. Zhang, Z. Guo, G. Lu, D. Zhang, and W. Zuo. An online system of multispectral palmprint verification. *Instrumentation and Measurement, IEEE Transactions on*, 59(2):480–490, Feb 2010.

[23] W. Zhao, R. Chellappa, P. J. Phillips, and A. Rosenfeld. Face recognition: A literature survey. *ACM Comput. Surv.*, 35(4):399–458, Dec. 2003.